Optical and Quantum Electronics (2024) 56:951
https://doi.org/10.1007/s11082-024-06930-6

Hydrophobic nickel doped Co_3O_4 sprayed thin films as solar absorber

Younes Nezzari[1] · Warda Darenfad[1] · Kamel Mirouh[1] · Noubeil Guermat[2] · Nadir Bouarissa[3] · Rayene Merah[1]

Received: 21 February 2024 / Accepted: 1 April 2024

Abstract

As part of this study, we elaborated and characterized samples of thin layers of cobalt oxide, doping them with different concentrations of nickel (2%, 4% and 6%). These films were deposited on ordinary glass substrates at a temperature of 400 °C, with a deposition time of 5 min, using the spray pyrolysis technique. The main objective of this research was to explore the influence of nickel doping on the physical properties of cobalt oxide. The results obtained by Raman spectroscopy confirmed the presence of Co^{+2} cations located in tetrahedral sites and Co^{+3} in octahedral sites, thus validating the spinel-type cubic structure. Morphological analysis revealed that the incorporation of nickel into the Co_3O_4 thin films, synthesized by spray pyrolysis, resulted in a significant transformation of the porous surface morphology. This transformation resulted in the transition from a porous structure to a dense and uniform configuration, characterized by nanoflower grains. Analyzes by EDS spectrometry revealed peaks associated with the elements Co and O, thus confirming the composition of the films. An improvement in the durability and overall performance of the solar device in humid environments by obtaining the hydrophobic character (CA = 99°) for the Co_3O_4/6%Ni film. The transmittance decreased with increased as a function of Ni concentration. Optical studies show direct band gaps E_{g1} and E_{g2} varying between 1.41 and 1.3 eV and between 2.09 and 1.99 eV respectively. Notably, the electrical resistivity experienced a significant decrease from 28.39 to 0.178 Ω.cm for the undoped and 2% Ni-doped films, respectively. However, for Ni concentrations ≥ 4%, the electrical resistivity increased from 3.47 to 10.2 Ω cm.

Keywords Thin films · Spray pyrolysis · Ni-doped Co_3O_4 · Hydrophobic · Solar absorber

✉ Warda Darenfad
daranfed.warda@umc.edu.dz

[1] Thin Films and Interfaces Laboratory (LCMI), University of Constantine 1, 25000 Constantine, Algeria

[2] Department of Electronics, Faculty of Technology, University of M'sila, P.O. Box 166 Ichebilia, 28000 M'sila, Algeria

[3] Laboratory of Materials Physics and Its Applications, University of M'sila, 28000 M'sila, Algeria

Published online: 24 April 2024

1 Introduction

In our world teeming with technological materials, metal oxides occupy a leading position in multiple scientific and technological fields. These compounds, among the most widespread in the earth's crust, result from the oxidation of metals in reaction with oxygen in the air, at specific temperatures and pressures. Although various metal oxides exist, such as those of the alkali, alkaline earth, and rare earth metals, transition metal oxides (TMOs) are of particular interest due to their unique electrical and magnetic properties. Oxides, influenced by the electronic configuration of metal ions and structural geometries, can exhibit insulating or semiconducting behaviors. Among the conductive metal oxides, cobalt oxide (Co_3O_4), belonging to the family of transition metal oxides, stands out as a p-type semiconductor. Researchers are investing intensively in improving the physical properties of Co_3O_4 to broaden its scope of application. Dopants prove to be key players, offering the possibility of being incorporated into the Co_3O_4 matrix. Several dopants, such as Mn (Soltani et al. 2022), Mo (Khalid et al. 2021), Sb (Ali et al. 2021), Zr (Yang et al. 2021), and Ni (Lavanya et al. 2023; Lakehal 2018), are associated with Co_3O_4 by various researchers, revealing a significant improvement in electrical conductivity. In this study, the choice of nickel as a transition metal for doping is explained by several factors. First, the ionic radii of nickel are almost equivalent to those of cobalt, which allows a modest concentration of Ni to improve crystallinity, adjust the energy gap, and optimize the electrical attributes of cobalt (Cheng et al. 2021). Second, the replacement of cobalt by nickel offers the possibility of forming oxygen vacancies, favorably impacting photodetection performance (Guo et al. 2020). Finally, nickel stands out as an economical and less toxic dopant (Lavanya et al. 2023). Taking all of these elements into consideration, nickel doping appears to be a promising avenue for improving the physical properties of Co_3O_4. For example, the study by Lakehal (2018) examined the impact of nickel-doped Co_3O_4, concluding that Ni increases conductivity properties. Similarly, the influence of Ni doping concentration on the wettability properties of cobalt oxide was investigated by Nayana et al. (2019), revealing a naturally hydrophobic surface with water contact angles (WCA) of 92°. Hydrothermal synthesis and annealing treatment were employed by Li et al. (2020) to produce Ni-doped Co_3O_4 (2 wt%, 4 wt%, 6 wt% and 8 wt%). Their results indicated that 4 wt%Ni-Co_3O_4 was more hydrophilic (WCA = 22°). According to the literature, nickel-doped Co_3O_4 plays a prominent role in many scientific applications, such as gas sensors (Cheng et al. 2021), electrocatalysis (Li et al. 2020), and Li-ion batteries (Zawar et al. 2021). Methods for preparing Co_3O_4:Ni thin films have achieved remarkable precision, with the spray pyrolysis method, employed in this study, standing out among them. The main objective of this research is to develop thin films of the hydrophobic nature of nickel-doped Co_3O_4 for use as absorber layers in solar cells. This approach involves an in-depth study of the effect of nickel doping (2%, 4% and 6%) on the properties of cobalt oxide, deposited on ordinary glass substrates by spray pyrolysis, in order to understand in detail the variations of their structural, morphological, optical and electrical properties.

2 Experimental procedure

For the preparation of thin layers of cobalt oxides doped with nickel, we have used, in our work, cobalt nitrate ($Co(NO_3)_2{\cdot}6H_2O$) and nickel nitrate as sources of cobalt. Solutions are prepared by mixing 0.291 g of cobalt nitrate with nickel doping percentages (2%, 4% and 6%) in 20 ml of distilled water, prepared at room temperature. The mixture solution was stirred at room temperature for 30 min to obtain a homogeneous solution. For the sets of samples prepared, the distance between the atomizer and the substrate was consistently maintained at 17 cm. Compressed air, serving as the carrier gas, and the precursor were supplied to a spray nozzle at a constant atomization pressure of 1 bar. The substrate temperature was also kept constant at 400 °C. The following diagram summarizes the experimental deposition procedure used to develop our films (Fig. 1):

The measurement of the thickness of our films is done using a DECTAK3 type profilometer. Raman spectra were carried out with a laser source with a wavelength of 473 nm using a HORIBA lab Ram HR Evolution type Raman spectrometer. The surface morphology and microstructure were investigated by scanning electron microscope (SEM) embedded with an Energy Dispersive x-ray (EDS) system (FEI Quanta 450 FEG). The values of the contact angle for each deposit were obtained after 5 s with a drop of distilled water of volume = 5 µl. The optical properties were obtained using UV–VIS–NIR spectrophotometer (Shimadzu, Model UV–3101 PC) in the wavelength range from 300 to 1000 nm. The electrical properties (resistivity, charge carrier density and *mobility) were characterized at room temperature by the Hall Effect method.

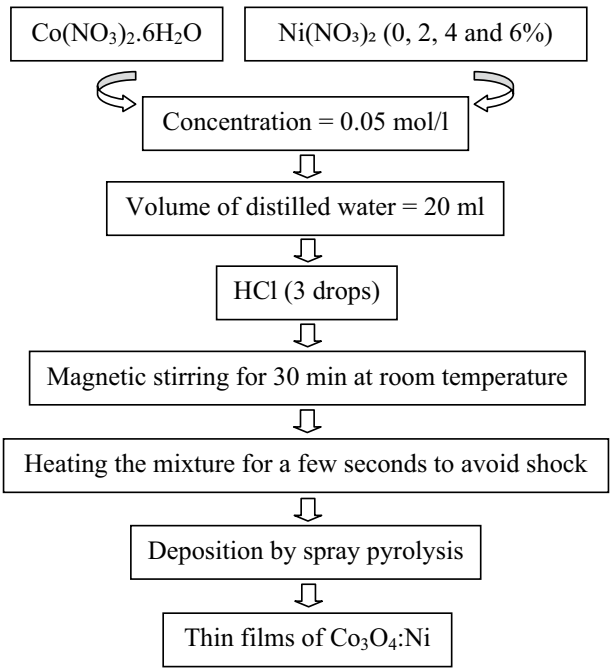

Fig. 1 Processing steps used for undoped and Ni doped film deposition

3 Results and discussion

In Fig. 2, we present the Raman spectra of films produced with varying concentrations of nickel (2%, 4%, and 6%). The spectra clearly show the presence of five distinct modes, corresponding to vibration modes of the Co–O bond. These Raman peaks are located at approximately 190, 467, 512, 602, and 670 cm^{-1}, corresponding to the F_{2g}, E_g, and A_{1g} phonon symmetries. These vibrations arise from the motion of Co^{+2} and Co^{+3} cations within tetrahedral and octahedral sites of the cubic lattice, confirming the single-phase cubic spinel structure of Co_3O_4 (Darenfad et al. 2024). Furthermore, no phases corresponding to nickel compounds were detected in the spectra, consistent with findings in existing literature (Zhang et al. 2024a; Chai et al. 2021). Additionally, the incorporation of Ni^{+2} ions, with an ionic radius of 0.069 nm, results in an elongation of the bond length between Co^{+3} ions (ionic radius of 0.061 nm) and O^{-2} ions, as well as a reduction in binding energy. This specifically leads to a redshift of the A_{1g} peak (Zhang et al. 2024b).

When comparing the Raman spectra of pure Co_3O_4 with those of Co_3O_4 doped with varying concentrations of nickel, a significant reduction in peak intensities, particularly the A_{g1} peak, is noticeable. This peak shows a shift towards lower frequencies as the nickel concentration increases, as shown in Fig. 3. This shift can be attributed to a slight decrease in particle size, a hypothesis supported by previous research (Ali et al. 2021). Additionally, this behavior aligns with the confinement effect observed in optical phonons (Yang et al. 2021). It is important to note that the substitution of Co^{+2} and Co^{+3} cations with Ni^{+2} cations within the cobalt oxide network structure could have caused localized alterations. These alterations likely increased defects within the crystal lattice of Co_3O_4, leading to a distortion in the Co_3O_4 crystal lattice and a reduction in its spatial symmetry. Li et al. (2020), in their study on the effect of Ni on Co_3O_4, confirmed the incorporation of Ni^{+2} cations into the cobalt oxide lattice. Zhang et al. (2024a) deposited Co_3O_4 thin films using a thermal treatment method with various Ni doping concentrations. They observed that as the Ni dopant concentration increased, the position of the A_{g1} mode systematically shifted to higher wavenumbers. This indicates that the introduction of Ni into the Co_3O_4 lattice

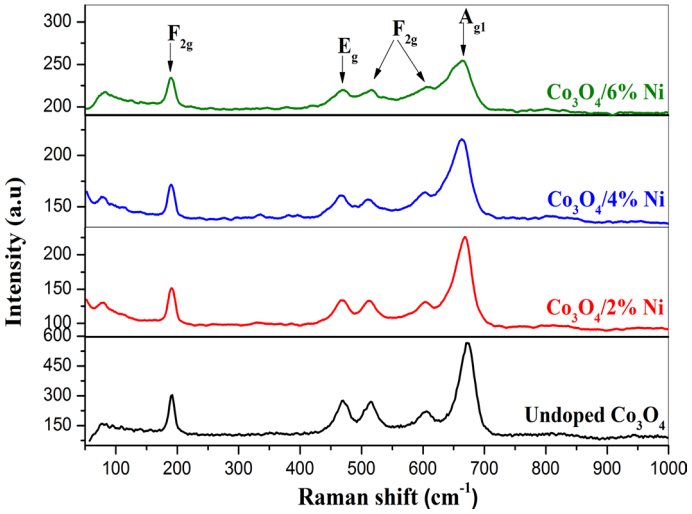

Fig. 2 Raman spectra of cobalt oxide as a function of nickel concentration: **a** 0% and **b** 2%, 4% and 6%

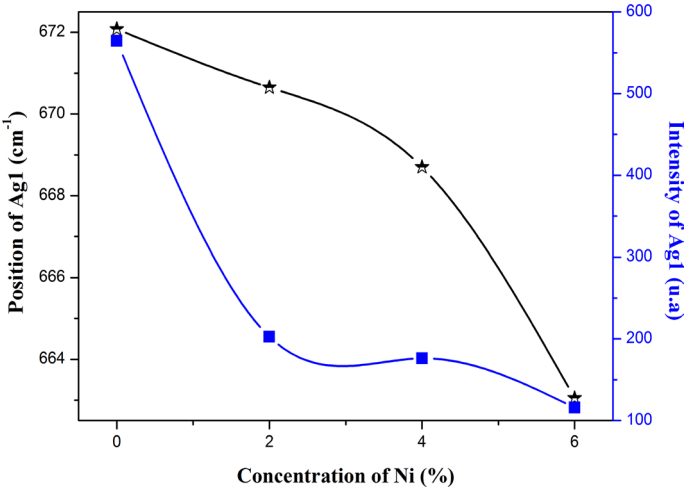

Fig. 3 Position and intensity of A_{g1} peak as a function of %Ni concentration

had a noticeable impact on the octahedral coordination environment of Co^{+3}, leading to distortions in the lattice structure and the formation of lattice defects (Zhang et al. 2024a).

The SEM micrographs of undoped and Ni-doped Co_3O_4 thin films are presented in Fig. 4a–d, respectively. The visual representation presented in the Fig. 4a highlights the thin film of undoped Co_3O_4, where grains of nanometric dimensions are dispersed relatively homogeneously, with the presence of pores. When we observe an increase in the nickel concentration, going from 2 to 4%, we notice an influence on the morphology of the film, leading to the formation of pores of variable sizes and irregular shapes, as illustrated in Fig. 4b, c. Recently Albargi et al. (2021) observed a similar type of morphology in Sn-doped Co_3O_4 thin films. At an even higher nickel concentration (6%), as shown in Fig. 4d, a significant transformation of the surface is observed, adopting a dense and uniform configuration. The grains then take the form of nanoflowers which completely cover the substrate. The outer arrangement of this structure, meticulously crafted for its role in photovoltaic applications as an absorbing film.

The chemical composition of Co_3O_4 and Co_3O_4:Ni films deposited on glass substrates was studied using EDX. In Fig. 5a, we have reported the spectrum of the undoped Co_3O_4 film, where the peaks relative to the elements of O and Co are observed. The similar peaks of O and Co are also observed in the spectrum of Fig. 5b relating to the Co_3O_4 film doped with 2%Ni, we note the emergence of the small peaks corresponding to Ni.

Figure 6 represents the static images of the water drop on glass/Co_3O_4/%Ni substrates for four Ni concentrations (0%, 2%, 4% and 6%) measured at room temperature. In order to avoid any effect of water liquid evaporation, all contact angle (CA, θ) measurements are performed 5 s after the deposition of a drop of water on our films.

The variation of the contact angle as a function of doping is illustrated in Fig. 7. According to Fig. 7, we notice a variation in the contact angle between 58° and 99° depending on the nickel concentration. In addition, a hydrophilic character ($CA < 90°$) obtained for the 100% Co_3O_4, Co_3O_4/2%Ni and Co_3O_4/4%Ni films with a low value of θ for the film doped with 2%Ni, indicating good adhesion and cohesion of water molecules on the surface due to the porosity of the films produced. On the other hand, we also have a hydrophobic

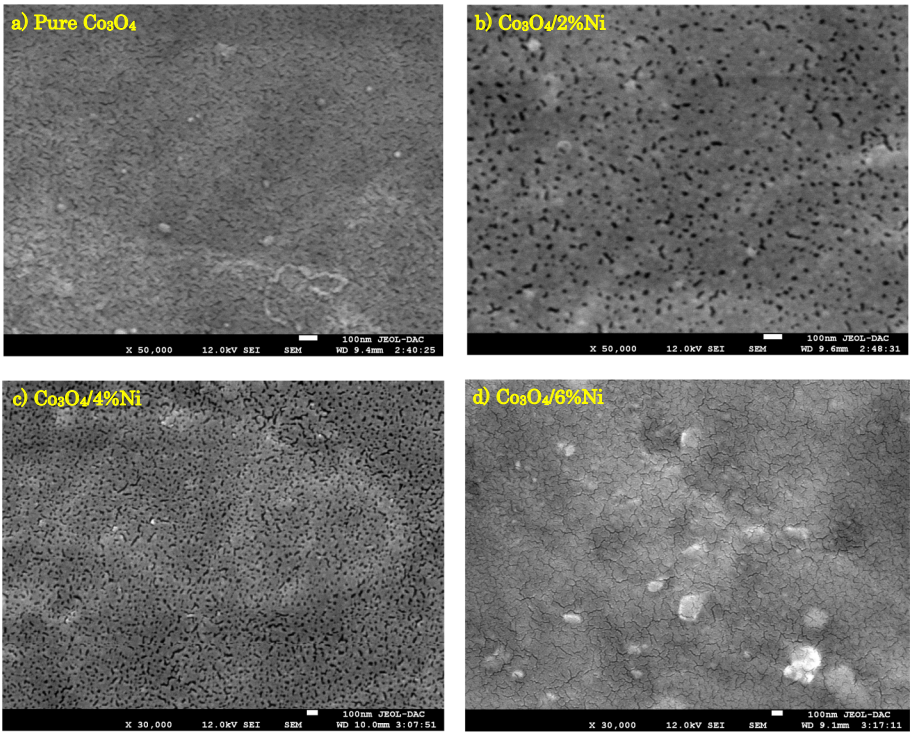

Fig. 4 SEM images of Co_3O_4 films deposited with different Ni doping rates: **a** 0%, **b** 2%, **c** 4% and **d** 6%

character (CA > 90°) for the 6%Ni doped film, indicating less interaction of the surface with the water drop. The wettability properties are affected by the addition of nickel with cobalt oxide. This result is in good agreement with the SEM analysis. This behavior was observed by the work of Darenfad et al. (2023b) studies cobalt-doped CuO films produced by spray pyrolysis. This change from hydrophilic to hydrophobic nature depending on doping is probably due to the available pore size, pore radius and their distribution (Darenfad et al. 2023b). Therefore, the porous Co_3O_4/2%Ni film has a high adsorption capacity compared to other films developed, which makes it possible to improve the sensitivity or reactivity of the sensitive layer of gas sensors. On the other hand, the hydrophobic nature obtained for the Co_3O_4/6%Ni film is a very important characteristic: (i) for the absorbent layer in the manufacture of thin film solar cells. (ii) to improve the durability and overall performance of the solar device in humid environments.

The optical properties of undoped and doped Co_3O_4 thin films were characterized using a computer-driven dual-beam spectrophotometer, working in the UV–Visible range from 300 to 1000 nm. The spectra obtained show the variation of the transmittance (T%) as a function of the wavelength (λ) in the range of 300–1000 nm (Fig. 8). From Fig. 8, high values of transmittance in the infrared (IR) region and small values of transmittance in the visible region are observed for different concentrations of nickel. The same result has been observed by other researchers (Abdelmoneim et al. 2021; Shkir et al. 2022). We also always observe in Fig. 8, the presence of two absorption bands in the spectra of the transmittance between 400 and 600 nm and between 700 and 900 nm, which are attributed to

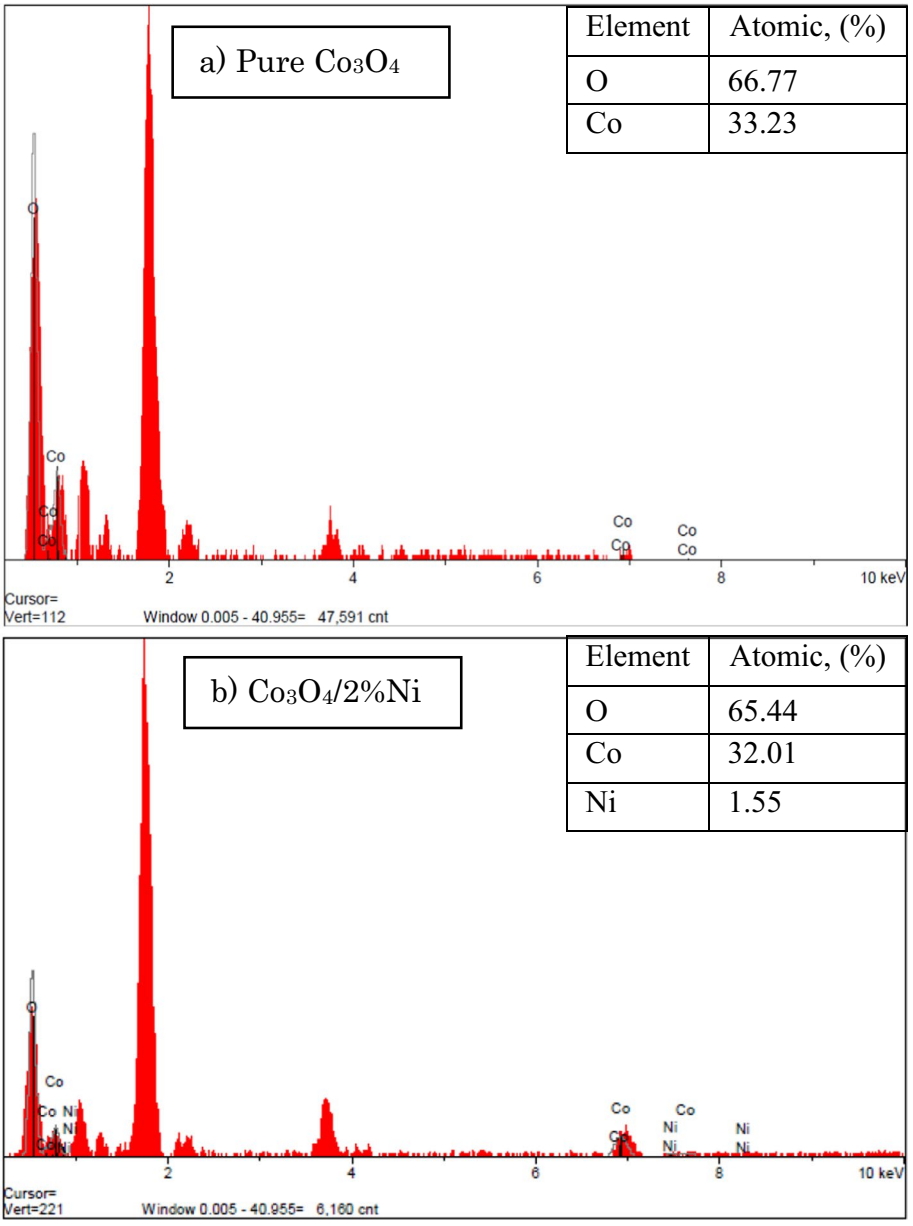

Fig. 5 EDX spectra of Co_3O_4 film: **a** pure and **b** doped 2%Ni

charge transfer ($O^{-2} \rightarrow Co^{+2}$) and ($O^{-2} \rightarrow Co^{+3}$) in processed films. This indicates the presence of two optical gaps, in agreement with the literature (Lavanya et al. 2023).

Furthermore, in order to evaluate the impact of doping on transmission, the analysis of the transmission spectra of thin layers of Co_3O_4, with and without nickel doping, reveals absorbing characteristics, accompanied by a shift towards longer wavelengths. It

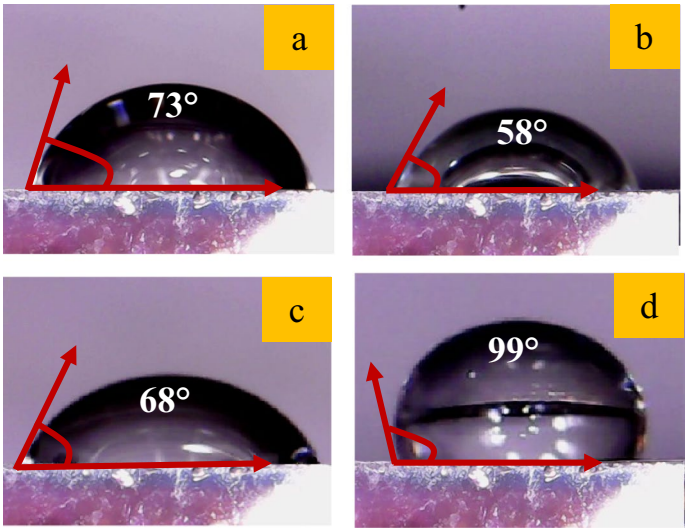

Fig. 6 Images of the contact angle for a thin film of Co_3O_4 as a function of nickel: **a** pure, **b** 2%, **c** 4% et **d** 6%

Fig. 7 Variation of the contact angle for a thin film of Co_3O_4 as a function of nickel

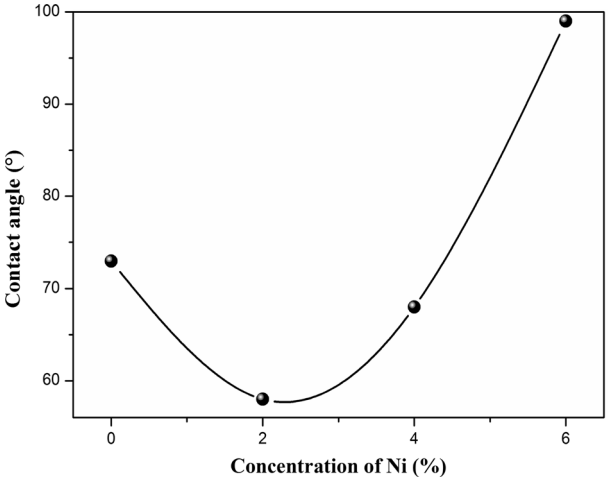

is important to note that the transmission shows a decrease proportional to the increase in nickel doping concentration. This phenomenon is likely due to the increase in the thickness of our films, which transitioned from 300, 272, 312 to 420 nm with the addition of Ni to Co_3O_4, consistent with the Beer-Lambert law ($e^{-\alpha d}$), or it could result from the black color of our deposited films. Additionally, as the doping concentration increased, a significant decrease in the transmittance values was observed in the UV–Visible spectra. This observation leads to the conclusion that the introduction of doping rendered Co_3O_4 more optically dense, as the increasing absorption levels serve as an indicative measure of optical density (Alem et al. 2023).

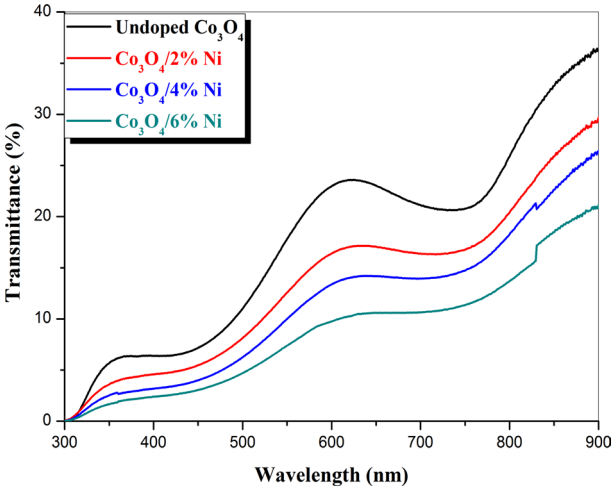

Fig. 8 Transmission spectra of undoped and Ni-doped Co_3O_4 thin films

From the spectra of transmittance we deduced the optical gaps (Eg) of our films according to the Tauc method (Daranfed et al. 2020; Darenfad et al. 2023a; Khalfallah et al. 2020), the value of the optical gap corresponds to the direct transitions was deduced from the curve of the variation of $(\alpha h\nu)^2$ as a function of $h\nu$ as shown in Fig. 9.

Through the curves of Fig. 9, we find the variations of the two optical gaps as a function of Ni concentrations. The double bands spotted in the current samples provide indications of the occurrence of an interband transition within the spinel configuration of Co_3O_4. Miedzinska et al. (1987) also identified a similar type of transition within Co_3O_4 films by applying a combined atomic orbital theory approach. According to their conclusions, the minimum band gap E_{g1} is related to the $O^{-2}\rightarrow Co^{+3}$ charge transfer process, while the maximum band gap E_{g2} is associated with the excitation from valence to the conduction band, illustrating the $O^{-2}\rightarrow Co^{+3}$ charge transition (Manickam et al. 2017).

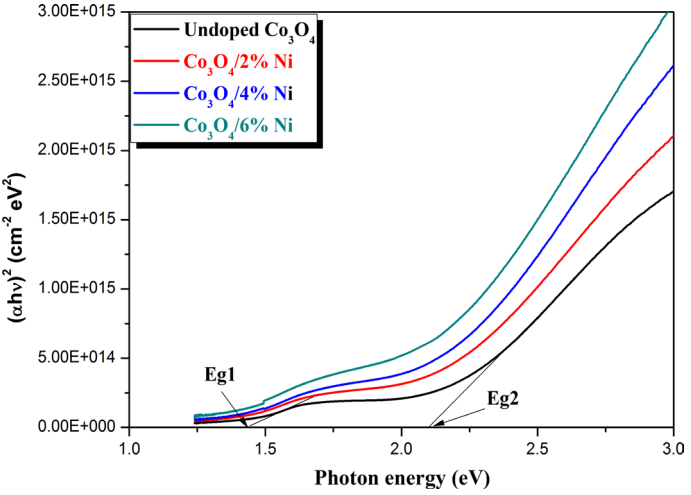

Fig. 9 Determination of the energy gap by the extrapolation method from the variation $(\alpha h\nu)^2$ as a function of $(h\nu)$ for different Ni concentrations

Figure 10 shows the evolution of two optical gaps (E_{g1} and E_{g2}) for our films. In accordance with Fig. 10, the values of these two gaps, E_{g1} and E_{g2}, experience a decrease during nickel doping. This reduction in the gaps with increasing doping rate can be primarily attributed to the distortions caused by Ni ions, which generate impurity energy levels within the band gaps of Co_3O_4 (Ali et al. 2013), in good agreement with the Raman spectra. This structural change is a result of the introduction of impurities through doping, leading to the creation of impurity energy levels, specifically acceptor levels, within the optical gap of the material. These impurity energy levels contribute to the observed decrease in the optical gap values, highlighting the significant impact of nickel doping on the optical properties of our films. The same result was observed by Lakehal (2018), who studied Co_3O_4 films deposited using the sol–gel technique with Ni concentrations varying between 3 and 9%, and annealed at 400 °C. The decrease in the optical gaps with increasing concentration is attributed to the decrease in the crystallite size (Zribi et al. 2023). In summary, our results indicate that the calculated optical band gaps fall within an optimal range for solar cells, making them promising candidates for use as absorber layers. Particularly, the film elaborated with a 6% Ni exhibits optical band gaps of $E_{g1} = 1.3$ eV and $E_{g2} = 1.99$ eV, which closely align with the requirements for solar cells as they correspond well with the solar spectrum.

The Urbach energy (E_U, disorder) gives the extent of the tail of localized states in the optical band space, which has been considered as a useful parameter to assess the degree of structural disorder (Daranfed et al. 2020). Therefore, one can calculate the Urbach energy of the thin films of the undoped and nickel doped cobalt oxide from the Urbach law (Guermat et al. 2021; Darenfad et al. 2021). By plotting ln(α) as a function of hυ, we can determine the value of the Urbach energy as illustrated in Fig. 11.

Figure 12 shows the evolution of two disorders (E_{U1} and E_{U2}) in cobalt oxide films as a function of Ni content. As shown in Fig. 12, there is an increase in two disorders upon the introduction of nickel dopant into the Co_3O_4 network. This behavior is likely caused by the increase in the number of cobalt and nickel atoms in interstitial positions

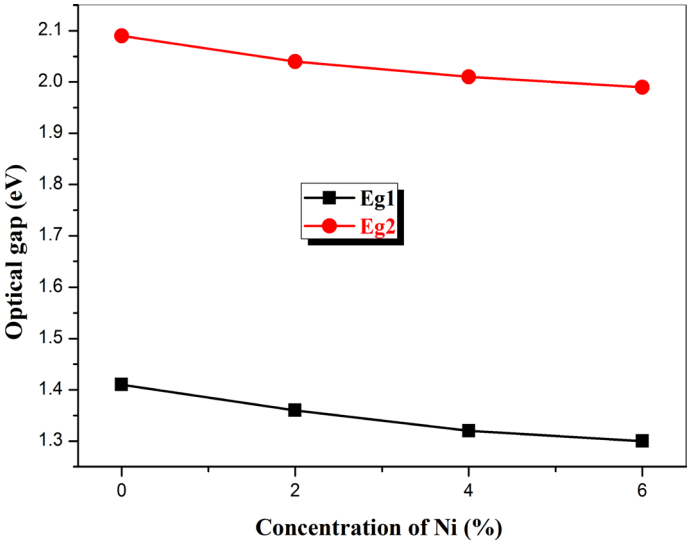

Fig. 10 Variation of the two optical gaps E_{g1} and E_{g2} of %Ni doped Co_3O_4 thin films

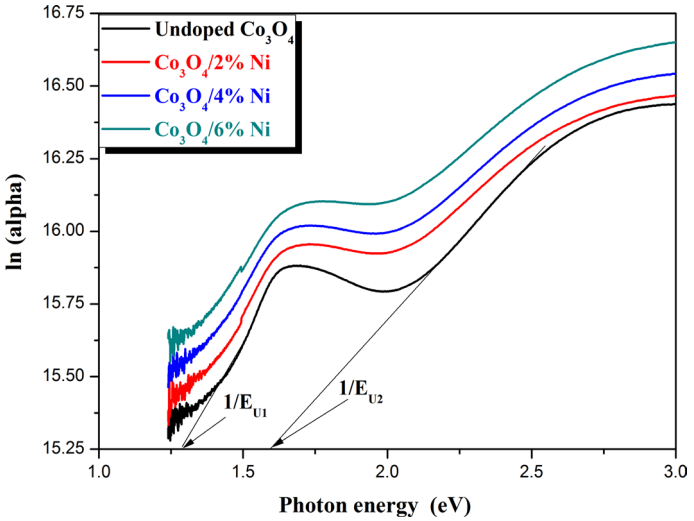

Fig. 11 Determination of disorder by extrapolation from the variation of ln(α) as a function of hυ

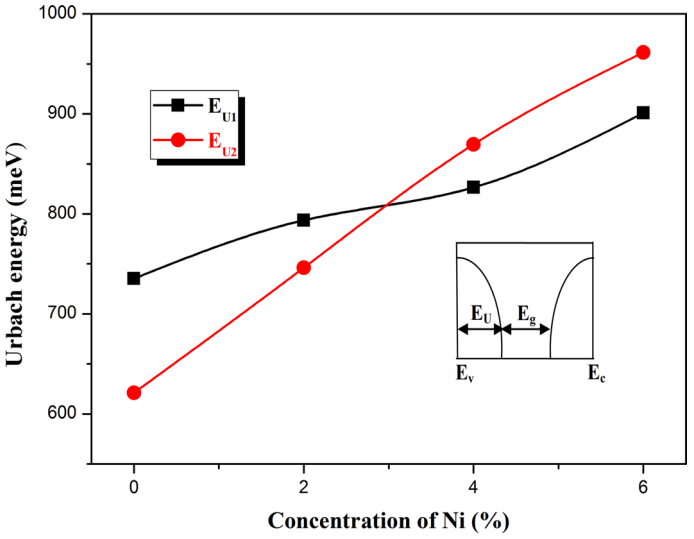

Fig. 12 Variation of two Urbach energies (E_{U1} and E_{U2}) of our films

with increasing thickness. It is important to note that at high growth rates (growth in thickness), atoms may not have sufficient time to reorganize and occupy stable and favorable sites, which results in the appearance of a large density of structural defects characterized by a strong disorder in the network (Behzad et al. 2018). Consequently, the presence of a high density of localized levels within the energy gap resulting from the presence of crystal defects inside the thin layer (Guermat et al. 2021). An increase in Urbach energy is accompanied by a reduction in the optical band gap (as depicted in

inset Fig. 12). This suggests that the variation of the optical gap is governed by the disorder in the film lattice.

To evaluate various parameters such as electrical resistivity (ρ), mobility (μ) and carrier concentration, we performed Hall effect measurements. These measurements initially indicate that our thin films are p-type semiconductors.

Figure 13 represents the different electrical parameters of our films (pure and nickel-doped Co_3O_4). According to the data in Fig. 13, there is a decrease in electrical resistivity up to 0.178 Ω cm when the nickel concentration reaches 2%. This reduction in electrical resistivity is likely attributable to the increase in the number of charge carriers, as shown in Fig. 13. The increase in growth rate results in the formation of disorder in the crystal lattice, as visualized in Fig. 12. This phenomenon leads to the emergence of defects such as cation or oxygen vacancies in interstitial sites. These defects act as doping impurities within the lattice (Uozumi et al. 1997), thus inducing an increase in the carrier concentration and, consequently, an increase in electrical conductivity. Furthermore, with increasing nickel concentration, increased substitution of cobalt atoms with nickel cations, which act as atom acceptors, is observed. This substitution causes an increase in the number of vacancies within the valence band, which leads to an increase in the density of this band. Darenfad et al. (2024) also observed a similar result during their study of Co_3O_4 films deposited by spray pyrolysis, varying the deposition time. This observation is likely due to an increase in the adsorbed oxygen content near the surface of the film. Furthermore, in ambient conditions, Co_3O_4 films adsorb oxygen from the air, resulting in the creation of oxygen-rich surface states. These surface states facilitate the excitation of electrons from the valence band to the conduction band, thereby leading to the generation of additional holes within the p-type Co_3O_4 crystallites (in addition to those induced by the non-stoichiometry of the oxygen lattice). Furthermore, the increase in electrical resistivity observed in the doping range from 4 to 6%Ni can be explained by three distinct phenomena. Firstly, there might be a reduction in the density of charge carriers (holes) responsible for electrical

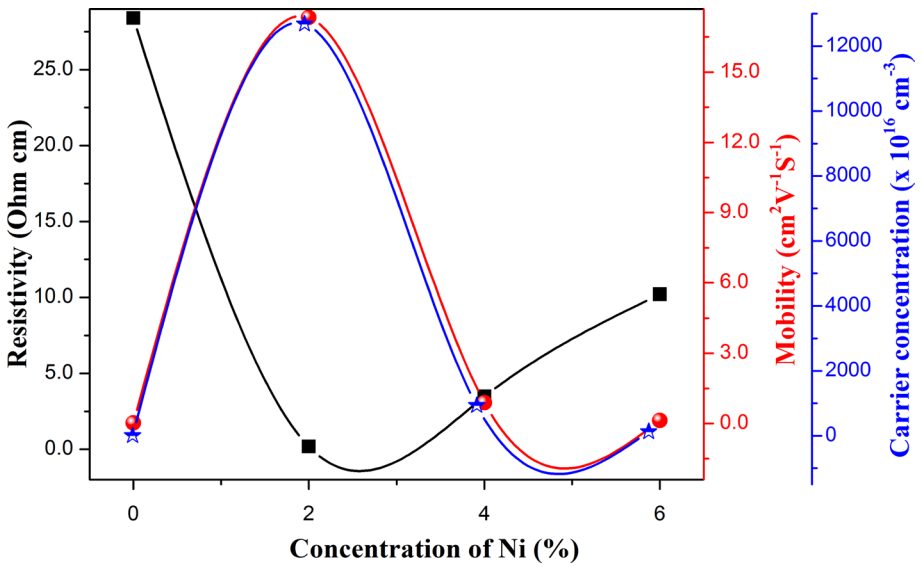

Fig. 13 Variation of resistivity (ρ), mobility (μ) and carrier concentration (n) of pure and Ni-doped Co_3O_4 films

conduction, as shown in Fig. 13. This reduction could stem from interactions between doping impurities and the crystal structure of Co_3O_4, or compensation effects that reduce the number of carriers available for conduction. Secondly, this decrease can also be attributed to a reduction in the mobility of charge carriers (Fig. 13). Accumulated interactions between charge carriers and doping impurities can hinder their mobility. Lastly, the increase in electrical resistivity is also linked to a reduction in the density of oxygen adsorbed on the surface of Co_3O_4:Ni. These findings are supported by observations from scanning electron microscopy (SEM) and contact angle measurements.

4 Conclusions

In this work we study the influence of the addition of Ni on the structural, morphological, optical and electrical properties of cobalt oxide. We then carried out analyzes on the samples produced by different characterization techniques such as: Raman spectroscopy, SEM, contact angle, UV–Visible spectroscopy and the Hall effect. Raman spectroscopy analysis showed that the deposited films have a spinel-type cubic structure. The morphological analysis emphasizes a notable consistency in the surface structure of the film, showcasing a gradual transformation of the grains into a distinctive nanoflower configuration as the doping concentration rises. The observed contact angles for undoped, Co_3O_4:2%Ni, and Co_3O_4:4%Ni are all below 90°, confirming the hydrophilic nature of these films. Additionally, the film doped with 6% Ni exhibits a hydrophobic character, evident from the contact angle exceeding 90° (CA = 99°). The transmittance of our fabricated films decreases as the doping concentration increases. The film prepared with a concentration of 6% Ni exhibits an optical band gaps of $E_{g1} = 1.3$ eV and $E_{g2} = 1.99$ eV, an essential value for solar cells due to its close conformity with the solar spectrum. In addition, it has a maximum resistivity of around 10.2 Ω cm. To conclude, this study has clearly demonstrated that the increase in the doping rate constitutes a crucial parameter which substantially influences the physical properties of Co_3O_4 films. These properties demonstrate that the Co_3O_4 film, which is deposited in particular 6%Ni, constitutes a promising material as an absorbent layer in photovoltaic applications.

Acknowledgements This work is supported by the Research Project University Formation (PRFU) of Algerian ministry of high education and scientific research (No. A10N01UN280120220009) entitled 'Study, elaboration and characterization of the effect of doping and co-doping on the properties of oxides of transition metals for optoelectronic applications'.

Author contributions YN, WD, KM, NG, NB and RM wrote the main manuscript text and YN prepared all figures. All authors reviewed the manuscript.

Data availability No datasets were generated or analysed during the current study.

Declarations

Conflict of interest The authors declare no competing interests.

References

Abdelmoneim, A., Naji, A., Wagenaars, E., Shaban, M.: Outstanding stability and photoelectrochemical catalytic performance of (Fe, Ni) co-doped Co_3O_4 photoelectrodes for solar hydrogen production. Int. J. Hydrogen Energy **46**, 12915–12935 (2021). https://doi.org/10.1016/j.ijhydene.2021.01.113

Albargi, H., Marnadu, R., Sujithkumar, G., Alkorbi, A.S., Hassan, A., Shkir, M., Ahmad, U.: Deposition of nanostructured Sn doped Co_3O_4 films by a facile nebulizer spray pyrolysis method and fabrication of p-Sn doped Co_3O_4/n-Si junction diodes for Opto nanoelectronics. Sens. Actuator Phys. **32**, 113067 (2021). https://doi.org/10.1016/j.sna.2021.113067

Alem, A.F., Worku, A.K., Ayele, D.W., Wubieneh, T.A., Teshager, A.A., Kndie, T.M., Admasu, B.T., Teshager, M.A., Asege, A.A., Ambaw, M.D., Zeleke, M.A., Shibesh, A.K., Yemata, T.A.: Ag doped Co_3O_4 nanoparticles for high-performance supercapacitor application. Heliyon **9**, e13286 (2023). https://doi.org/10.1016/j.heliyon.2023.e13286

Ali, G.A.M., Fouad, O.A., Makhlouf, S.A.: Structural, optical and electrical properties of sol–gel prepared mesoporous Co_3O_4/SiO_2 nanocomposites. J. Alloys Compd. **579**, 606–611 (2013). https://doi.org/10.1016/j.jallcom.2013.07.095

Ali, F., Khalid, N.R., Tahir, M.B., Nabi, G., Shahzad, K., Ali, A.M., Kabli, M.R.: Capacitive properties of novel Sb-doped Co_3O_4 electrode material synthesized by hydrothermal method. Ceram. Int. **47**, 32210–32217 (2021). https://doi.org/10.1016/j.ceramint.2021.08.114

Behzad, H., Ghodsi, F.E., Peksu, E., Karaagac, H.: The effect of Cu content on structural, optical and photo-electrical properties of sol-gel derived $Cu_xCo_{3-x}O_4$ thin films. J. Alloys Compd. **744**, 470–480 (2018). https://doi.org/10.1016/j.jallcom.2018.02.114

Chai, G., Zhang, W., Liotta, L.F., Li, M., Guo, Y., Giroir-Fendler, A.: Total oxidation of propane over Co_3O_4-based catalysts: Elucidating the influence of Zr dopant. Appl. Catal. B **298**, 120606 (2021). https://doi.org/10.1016/j.apcatb.2021.120606

Cheng, P., Fan, D., Wang, Y., Gao, J., Xu, L., Wang, C., Lv, L., Xu, L., Zhang, B., Liu, B.: Gas sensor towards n-butanol at lowtemperature detection: hierarchical flower-like Ni-doped Co_3O_4 based on the solvent-dependent synthesis. Sens. Actuator. B Chem. **328**, 129028 (2021). https://doi.org/10.1016/j.snb.2020.129028

Daranfed, W., Guermat, N., Mirouh, K.: Experimental study in the effect of precursors in Co_3O_4 thin films used as solar absorbers. Ann. Chim.-Sci. Mat. **44**, 121–126 (2020). https://doi.org/10.18280/acsm.440207

Darenfad, W., Guermat, N., Mirouh, K.: A comparative study on the optoelectronic performance of undoped, Mg-doped and F/Mg co-doped ZnO nanocrystalline thin films for solar cell applications. J. Nano Electron. Phys. **13**, 06016 (2021). https://doi.org/10.21272/jnep.13(6).06016

Darenfad, W., Guermat, N., Mirouh, K.: Thoughtful investigation of ZnO doped Mg and co-doped Mg/Mn, Mg/Mn/ F thin films: a first study. J. Mol. Struct. **1286**, 135574 (2023a). https://doi.org/10.1016/j.molstruc.2023.135574

Darenfad, W., Guermat, N., Mirouh, K.: Effect of co-doping on structural, morphological, optical and electrical properties of p-type CuO films. J. Nano Electron. Phys. **15**, 06009 (2023b). https://doi.org/10.21272/jnep.15(6).06009

Darenfad, W., Guermat, N., Bouarissa, N., Satour, F.Z., Zegadi, A., Mirouh, K.: Improvement in optoelectronics and photovoltaic properties of p-Co_3O_4/n-ZnO hetero-junction: effect of deposition time of sprayed Co_3O_4 thin films. J. Mater. Sci. Mater. Electron. **35**, 162 (2024). https://doi.org/10.1007/s10854-023-11909-2

Guermat, N., Daranfed, W., Bouchama, I., Bouarissa, N.: Investigation of structural, morphological, optical and electrical properties of Co/Ni co-doped ZnO thin films. J. Mol. Struct. **1225**, 129134 (2021). https://doi.org/10.1016/j.molstruc.2020.129134

Guo, B., Ma, R., Li, Z., Luo, J., Yang, M., Wang, J.: Dual-doping of ruthenium and nickel into Co_3O_4 for improving the oxygen evolution activity. Mater. Chem. Front. **4**, 1390–1396 (2020). https://doi.org/10.1039/D0QM00079E

Khalfallah, M., Guermat, N., Daranfed, W., Bouarissa, N., Bakhti, H.: Hydrophilic nickel doped porous SnO_2 thin films prepared by spray pyrolysis. Phys. Scr. **95**, 095805 (2020). https://doi.org/10.1088/1402-4896/aba8c5

Khalid, N.R., Batool, A., Ali, F., Nabi, G., Tahir, M.B., Rafique, M.: Electrochemical study of Mo-doped Co_3O_4 nanostructures synthesized by sol–gel method. J. Mater. Sci. Mater. Electron. **32**, 3512–3521 (2021). https://doi.org/10.1007/S10854-020-05097-6

Lakehal, A.: Structural, optical and electrical properties of Ni-doped Co_3O_4 prepared via Sol-Gel technique. Mater. Res. **21**, 20170545 (2018). https://doi.org/10.1590/1980-5373-mr-2017-0545

Lavanya, S., Rajesh Kumar, T., Loyola Poul Raj, I., Vinoth, S., Rimal Isaac, R.S., Ganesh, V., Yahia, I.S., AlAbdulaa, T.H.: Enhanced structural, optical, and photo sensing properties of Ni-doped Co_3O_4 thin films prepared by nebulizer spray pyrolysis method. Phys. B Condens. Matter **649**, 414492 (2023). https://doi.org/10.1016/j.physb.2022.414492

Li, L., Xu, Q., Zhang, Y., Li, J., Fang, J., Dai, Y., Cheng, X., You, Y., Li, X.: Low Ni-doped Co_3O_4 porous nanoplates for enhanced hydrogen and oxygen evolution reaction. J. Alloys Compd. **823**, 153750 (2020). https://doi.org/10.1016/j.jallcom.2020.153750

Manickam, M., Ponnuswamy, V., Sankar, C., Suresh, R., Mariappan, R., Chandra bose, A., Chandrasekaran, J.: Structural, optical, electrical and electrochemical properties of Fe:Co_3O_4 fhin dilms for supercapacitor applications. J. Mater. Sci. Mater. Electron. **28**, 18951–18965 (2017). https://doi.org/10.1007/s10854-017-7849-7

Miedzinska, K.M.E., Hollebone, B.R., Cook, J.G.: An assignment of the optical absorption spectrum of mixed valence Co_3O_4 spinel films. J. Phys. Chem. Solids **48**, 649–656 (1987). https://doi.org/10.1016/0022-3697(87)90154-5

Nayana, K.O., Rangatha, S., Shubha, H.N., Panduranappa, M.: Effect of sodium lauryl sulphate on microstructure, corrosion resistance and microhardness of electrodeposition of Ni−Co_3O_4 composite coatings. Trans. Nonferrous Met. Soc. China **29**, 2371–2383 (2019). https://doi.org/10.1016/S1003-6326(19)65143-5

Shkir, M., Khan, A., Imran, M., Ajmal Khan, M., Zargar, R.A., Alshahrani, T., Deva Arun Kumar, K., Mohanraj, P., Chandekar, K.V., Al Faify, S.: Spray pyrolysis developed Nd doped Co_3O_4 nanostructured thin films and their structural, and opto-nonlinear properties for optoelectronics applications. Opt. Laser Technol. **150**, 107959 (2022). https://doi.org/10.1016/j.optlastec.2022.107959

Soltani, S., Rozati, S.M., Askari, M.B.: Ethanol gas sensing performance of spinel Mn: Co_3O_4 nanostructure thin film prepared by spray pyrolysis. Micro Nanostruct. **169**, 207343 (2022). https://doi.org/10.1016/j.micrna.2022.207343

Uozumi, G., Miyayama, M., Yanagida, H.: Fabrication of a CuO-infiltrated ZnO composite and its gas sensing properties. J. Mater. Sci. **32**, 2991–2996 (1997). https://doi.org/10.1023/A:1018653323658

Yang, G., Zhu, B., Fu, Y., Zhao, J., Lin, Y., Gao, D., Li, J.: High-valent Zirconium-doping modified Co_3O_4 weave-like nanoarray boosts oxygen evolution reaction. J. Alloys Compd. **886**, 161172 (2021). https://doi.org/10.1016/j.jallcom.2021.161172

Zawar, S., Ali, G., Afshan, N., Atiq, S., Mustafa, G.M., Hasnain, H., Iftikhar, F.J.: Ni-doped Co_3O_4 spheres decorated on CNTs nest-like conductive framework as efficiently stable hybrid anode for Na-ion batteries. Ceram. Int. **47**, 27854–27862 (2021). https://doi.org/10.1016/j.ceramint.2021.06.214

Zhang, Y., Huang, C., Lu, J., Cao, H., Zhang, C., Zhao, X.S.: Ni-modified Co_3O_4 with competing electrochemical performance to noble metal catalysts in both oxygen reduction and oxygen evolution reactions. Appl. Surf. Sci. **651**, 159241 (2024a). https://doi.org/10.1016/j.apsusc.2023.159241

Zhang, Z.Y., Gu, Y.J., Wen, W., Ye, Z.Z., Wu, J.M.: Excellent rate performance enabled by Ni-doping for Co_3O_4 nanosheet electrodes in supercapacitors. J. Power. Sources **591**, 233808 (2024b). https://doi.org/10.1016/j.jpowsour.2023.233808

Zribi, T., Essaidi, H., Billeh Bouzourâa, M., Diliberto, S., Ottapilakkal, V., Touihri, S.: The effect of tin doping on physical properties of cobalt oxide thin films. Optik **293**, 171428 (2023). https://doi.org/10.1016/j.ijleo.2023.171428